Synthesis, Structural Investigation, and Reactivity of Neutral and Cationic Bis(guanidinato)zirconium(IV) Complexes

Andrew P. Duncan, Sarah M. Mullins, John Arnold,* and Robert G. Bergman*

Department of Chemistry and Center for New Directions in Organic Synthesis (CNDOS), University of California, and Division of Chemical Sciences, Lawrence Berkeley National Laboratory, Berkeley, California 94720-1460

Received November 21, 2000

The mono(guanidinato) complex Cp(guan)$ZrCl_2$ (**1**; guan = η^2-(^{i}PrN)$_2$C(NMe_2)) was prepared by treatment of $CpZrCl_3$ (Cp = η^5-C_5H_5) with the in situ generated lithium guanidinate salt **2**. The dimethylamino group of **1** resists quaternization by alkylating and silylating reagents. Complex **1** undergoes ligand redistribution when treated with 2 equiv of MeLi, but reaction with 2 equiv of MeMgCl affords the dimethyl derivative Cp(guan)$ZrMe_2$ (**3**). Insertion of 2 equiv of diisopropylcarbodiimide into the Zr−N bonds of $(Me_2N)_2ZrCl_2(THF)_2$ produces the bis(guanidinato)zirconium dichloride complex $(guan)_2ZrCl_2$ (**4**). Alkylation of **4** with 2 equiv of MeLi or $PhCH_2MgCl$ affords the dialkyl derivatives $(guan)_2ZrMe_2$ (**5**) and $(guan)_2Zr(CH_2Ph)_2$ (**6**), respectively. Variable-temperature NMR experiments on **6** reveal a limiting C_2-symmetric solution structure at 253 K. Complex **5** undergoes reaction with electrophiles (Me_3SiOTf (OTf = OSO_2CF_3), $B(C_6F_5)_3$, $[Ph_3C][B(C_6F_5)_4]$) to yield stable products of methide abstraction: neutral complexes $(guan)_2Zr(OTf)_2$ (**7**) and $(guan)_2Zr(Me)OTf$ (**8**), base-free cationic alkyl salts $[(guan)_2ZrMe][MeB(C_6F_5)_3]$ (**9**) and $[(guan)_2ZrMe][B(C_6F_5)_4]$ (**10**), and the dinuclear methyl-bridged cation $[((guan)_2ZrMe)_2$-μ-$Me][B(C_6F_5)_4]$ (**11**). Complexes **1**, **4**−**7**, and **11** have been characterized by X-ray diffraction. Dinuclear cation **11** exhibits bridge−terminal methyl exchange on the NMR time scale at room temperature, with decoalescence observed at 224 K. Dibenzyl complex **6** undergoes reaction with $[Ph_3C][B(C_6F_5)_4]$ in CH_2Cl_2, yielding the cationic benzyl complex $[(guan)_2Zr(CH_2Ph)][B(C_6F_5)_4]$ (**15**). Spectroscopic data imply that the benzyl ligand of **15** adopts an undistorted monodentate coordination mode. Complexes **4**, **5**, and **10** were found to have low to moderate activities for the polymerization of α-olefins.

Introduction

Although metallocenes and their derivatives have provided stable platforms for many stoichiometric and catalytic organometallic transformations, the need for alternative ancillary ligands with diverse electronic and steric properties has recently been emphasized.[1−3] This effort has been especially evident in the field of homogeneous Ziegler−Natta catalysis.[2,4−8]

Group 4 alkyl salts ($[L_nM(R)](X)$ (M = Ti, Zr, Hf; R = H, alkyl; X = weakly coordinating anion) have been implicated as the actively propagating species in homogeneous Ziegler−Natta α-olefin polymerization catalysis, prompting intense synthetic and mechanistic investigations on these systems.[9] Although olefin coordination and enchainment occur at the cationic metal center, the nature of the cocatalyst/counteranion has also been found to strongly affect catalyst productivity.[10] Specifically, it has been shown that attenuation of ion-pairing interactions leads to higher catalyst activities.[11−16] It is not surprising, then, that some of the most active homogeneous Ziegler-type catalysts reported to date have utilized the extremely weakly coordinating tetrakis(pentafluorophenyl)borate ($B(C_6F_5)_4$) counteranion.[17−19]

(1) Togni, A.; Venanzi, L. M. *Angew. Chem., Int. Ed. Engl.* **1994**, *33*, 497.
(2) Gade, L. H. *Chem. Commun.* **2000**, 173.
(3) Edelmann, F. T. *Coord. Chem. Rev.* **1994**, *137*, 403.
(4) Britovsek, G. J. P.; Gibson, V. C.; Wass, D. F. *Angew. Chem., Int. Ed.* **1999**, *38*, 428. Because of the excellent coverage in this review, we have not duplicated many of its citations explicitly in this paper. References 5−8 provide examples of diverse ligand sets used recently in Ziegler−Natta type polymerizations.
(5) Younkin, T. R.; Connor, E. F.; Henderson, J. I.; Friedrich, S. K.; Grubbs, R. H.; Bansleben, D. A. *Science* **2000**, *287*, 460.
(6) Tshuva, E. Y.; Goldberg, I.; Kol, M.; Weitman, H.; Goldschmidt, Z. *Chem. Commun.* **2000**, 379.
(7) Vollmerhaus, R.; Rahim, M.; Tomaszewski, R.; Xin, S.; Taylor, N. J.; Collins, S. *Organometallics* **2000**, *19*, 2161.
(8) Shmulinson, M.; Galan-Fereres, M.; Lisovskii, A.; Nelkenbaum, E.; Semiat, R.; Eisen, M. S. *Organometallics* **2000**, *19*, 1208.
(9) Jordan, R. F. *Adv. Organomet. Chem.* **1991**, *32*, 325 and references therein.
(10) Chen, E. Y.; Marks, T. J. *Chem. Rev.* **2000**, *100*, 1391.
(11) Chen, Y.; Metz, M. V.; Li, L.; Stern, C. L.; Marks, T. J. *J. Am. Chem. Soc.* **1998**, *120*, 6287.
(12) Jia, L.; Yang, X.; Stern, C.; Marks, T. J. *Organometallics* **1997**, *16*, 842.
(13) Yang, X.; Stern, C. L.; Marks, T. J. *J. Am. Chem. Soc.* **1994**, *116*, 10015.
(14) Yang, X.; King, W. A.; Sabat, M.; Marks, T. J. *Organometallics* **1993**, *12*, 4254.
(15) Lancaster, S. J.; Walker, D. A.; Thornton-Pett, M.; Bochmann, M. *Chem. Commun.* **1999**, 1533.
(16) Bochmann, M. *Angew. Chem., Int. Ed. Engl.* **1992**, *31*, 1181.
(17) Stephan, D. W.; Guerin, F.; Spence, R. E. v. H.; Koch, L.; Gao, X.; Brown, S. J.; Swabey, J. W.; Wang, Q.; Xu, W.; Zoricak, P.; Harrison, D. G. *Organometallics* **1999**, *18*, 2046.
(18) Giardello, M. A.; Eisen, M. S.; Stern, C. L.; Marks, T. J. *J. Am. Chem. Soc.* **1995**, *117*, 12114.

10.1021/om000995u CCC: $20.00 © 2001 American Chemical Society
Publication on Web 03/30/2001

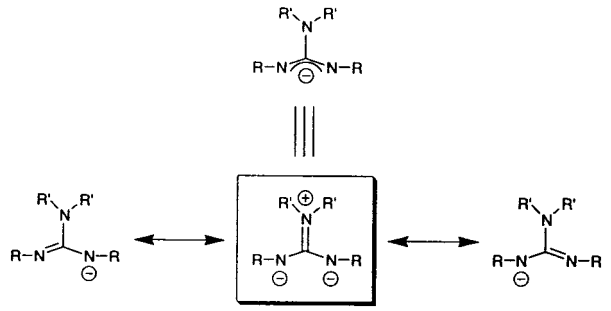

Figure 1. Resonance contributors for the guanidinate monoanion.

While these catalysts are highly active, Lewis base free $[L_nM-Me][B(C_6F_5)_4]$ salts generally lack sufficient thermal stability to be isolated in pure form.[7,12,17,20,21] We describe here the use of a bis(guanidinato) ancillary ligand set in the synthesis and characterization of neutral and cationic complexes of Zr, including the isolated and fully characterized base-free methyl cation $[(guan)_2Zr-Me][B(C_6F_5)_4]$.

Several research groups have recently reported complexes of both main group[22,23] and transition metals[24−32] with guanidinate monoanions ($[(RN)_2C(NR'_2)]^-$). The unique character of the chelating guanidinato (guan) ligand arises from the ability of the NR'_2 moiety to donate lone pair electron density to the central carbon atom of the chelate (provided that steric constraints allow for coplanarity of the dialkylamino group and the chelate ring) (Figure 1).[22] The resulting zwitterionic resonance structure places a formal negative charge on *both* nitrogen atoms used for metal−ligand bonding, thereby increasing their potential for electron donation to the metal. In a case where the metal center bears a positive charge, donation from the guanidinato ligand is anticipated to stabilize that charge by delocalizing it into the ligand framework (Figure 2). We anticipated that this donor effect might provide stabilization to an electronically unsaturated cationic Zr center sufficient to allow isolation and characterization of Lewis base-free $B(C_6F_5)_4$ salts of $[(guan)_2Zr-R]^+$ cations.

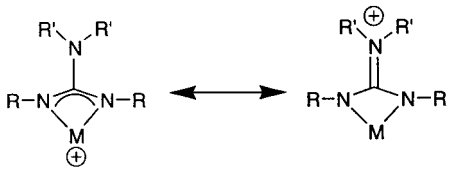

Figure 2. Resonance stabilization of a cationic metal center by a guanidinato ligand.

Results and Discussion

Synthesis, Structure, and Reactivity of Cp(guan)-ZrX_2 (X = Cl, Me) Derivatives. The synthesis of cationic zirconium alkyl complexes is often accomplished by alkide abstraction from neutral dialkylzirconium complexes using a strong Lewis acid. An initial concern about the (guanidinato)zirconium complexes was whether the Lewis basic dialkylamino group of the ligand would be inert under these conditions. Lone pair π-donation to the chelate from the NR'_2 group should lower its basicity, thereby rendering the ligand resistant to electrophilic attack at that site. Maximization of dialkylamino lone pair donation requires, as stated above, coplanarity of the NR'_2 moiety and the metal chelate. The ability of the ligand to achieve such a coplanar arrangement is controlled to a large degree by the steric demands of the ligand substituents. The choice of R′ = Me and R = ^{i}Pr for the guanidinato ligand used in this study represents a balance between minimization of intraligand steric interactions and steric protection of the metal center.

The basicity of the dimethylamino moiety and the extent of lone pair π-donation was assessed initially for the mono(guanidinato) complex $Cp(guan)ZrCl_2$ (**1**). Complex **1** was synthesized in 67% yield by treatment of $CpZrCl_3$ with the lithium guanidinate salt **2** (generated in situ from reaction of lithium dimethylamide and diisopropylcarbodiimide) in Et_2O (eq 1). Single crystals

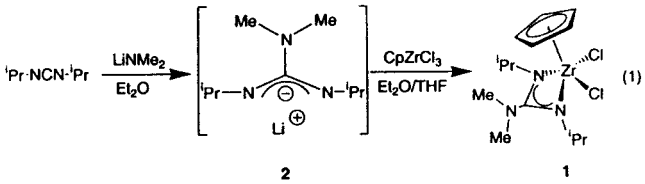

(1)

2 **1**

suitable for an X-ray diffraction study were obtained by vapor diffusion of pentane into a toluene solution of **1**. An ORTEP diagram depicting the molecular structure of **1** is shown in Figure 3. Representative bond lengths and angles are given in Table 1, and selected crystal and structure refinement data are shown in Table 2. The shortened C(1)−N(3) bond length of 1.373(4) Å (typical C−N single-bond length 1.42−1.45 Å) indicates some double-bond character between these atoms. This is likely the result of dimethylamino lone pair π-donation to the central carbon of the chelate ring and suggests that the dimethylamino group will display reduced Lewis basicity. Consistent with this hypothesis, complex **1** is unreactive toward alkylating and silylating agents (MeOTf, Me_3SiOTf, CH_3I) (Scheme 1). Thus, quaternization at N(3) is not observed.

Addition of 2 equiv of MeLi to **1** in Et_2O solution results in ligand redistribution: 0.5 equiv of Cp_2ZrMe_2 and 0.5 equiv of the bis(guanidinato) complex $(guan)_2$-

(19) Chien, J. C. W.; Llinas, G. H.; Rausch, M. D.; Lin, G. Y.; Winter, H. H. *J. Am. Chem. Soc.* **1991**, *113*, 8569.
(20) Horton, A. D.; de With, J.; van der Linden, A. J.; van de Weg, H. *Organometallics* **1996**, *15*, 2672.
(21) The methyl(decamethylthorocene) cation reported by Marks and co-workers is an important exception.[11,43]
(22) Aeilts, S. L.; Coles, M. P.; Swenson, D. C.; Jordan, R. F.; Young, V. G. *Organometallics* **1998**, *17*, 3265.
(23) Giesbrecht, G. R.; Shafir, A.; Arnold, J. *J. Chem. Soc., Dalton Trans.* **1999**, 3601.
(24) (a) Wood, D.; Yap, G. P. A.; Richeson, D. S. *Inorg. Chem.* **1999**, *38*, 8. (b) Note added in proof: For a very recent review of the coordination chemistry of guanidines and guanidinates, see: Bailey, P. J.; Pace, S. *Coord. Chem. Rev.* **2001**, 91.
(25) Tin, M. K. T.; Yap, G. P. A.; Richeson, D. S. *Inorg. Chem.* **1999**, *38*, 998.
(26) Tin, M. K. T.; Thirupathi, N.; Yap, G. P. A.; Richeson, D. S. *J. Chem. Soc., Dalton Trans.* **1999**, 2947.
(27) Robinson, S. D.; Sahajpal, A. *J. Chem. Soc., Dalton Trans.* **1997**, 3349.
(28) Holman, K. T.; Robinson, S. D.; Sahajpal, A.; Steed, J. W. *J. Chem. Soc., Dalton Trans.* **1999**, 15.
(29) Bailey, P. J.; Mitchell, L. A.; Parsons, S. *J. Chem. Soc., Dalton Trans.* **1996**, 2839.
(30) Thirupathi, N.; Yap, G. P. A.; Richeson, D. S. *Chem. Commun.* **1999**, 2483.
(31) Okamoto, S.; Livinghouse, T. *Organometallics* **2000**, *19*, 1449.
(32) Thirupathi, N.; Yap, G. P. A.; Richeson, D. S. *Organometallics* **2000**, *19*, 2573.

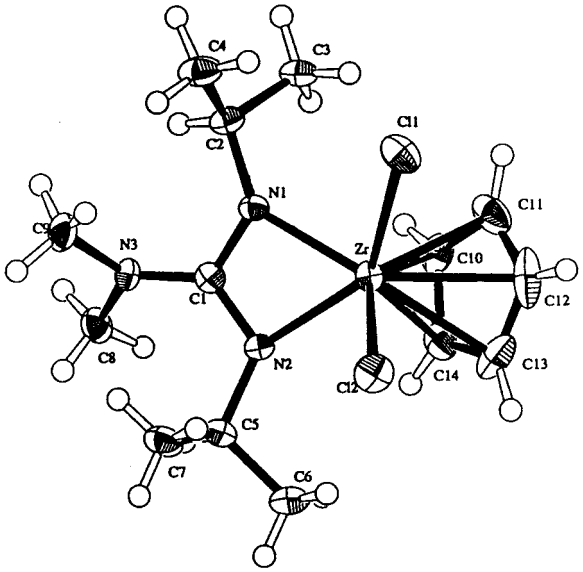

Figure 3. ORTEP diagram of $Cp(guan)ZrCl_2$ (**1**) showing non-hydrogen atom-numbering scheme (50% thermal ellipsoids).

Table 1. Metrical Data for $Cp(guan)ZrCl_2$ (1)

Selected Bond Lengths (Å)			
Zr−Cl(1)	2.4569(9)	Zr−Cl(2)	2.4247(9)
Zr−N(1)	2.166(3)	Zr−N(2)	2.225(2)
$Zr-Cp_{centroid}$	2.2120(3)	N(1)−C(1)	1.349(4)
N(2)−C(1)	1.331(4)	N(3)−C(1)	1.373(4)
Selected Bond Angles (deg)			
C(1)−Zr−Cl(2)	91.36(3)	N(1)−Zr−N(2)	60.43(9)
N(1)−C(1)−N(2)	111.1(3)	C(9)−N(3)−C(1)	121.0(3)
[N(1)−C(1−N(2)]/ [C(8)−C(9)−N(3)][a]	44.78		

[a] The angle between the planes of the chelate (N−C−N) and its dimethylamino substituent.

$ZrMe_2$ (vide infra), are observed by ^1H NMR spectroscopy (Scheme 1). However, alkylation with 2 equiv of MeMgCl in Et_2O affords the desired $Cp(guan)ZrMe_2$ product (**3**) in 61% yield (Scheme 1).

Synthesis and Structures of $(guan)_2ZrX_2$ Complexes (X = Cl, CH_3, CH_2Ph, OTf). Synthesis of the bis(guanidinato) complex $(guan)_2ZrCl_2$ (**4**) is accomplished by treatment of $(Me_2N)_2ZrCl_2(THF)_2$ with 2 equiv of diisopropylcarbodiimide (eq 2). Spectroscopically pure **4** is obtained in >90% yield simply by removal of solvent from the crude reaction mixture. Recrystallization from Et_2O gives analytically pure **4** in 54% yield. Similar insertion of carbodiimides into metal−amide bonds has been observed in related systems.[25,33] An ORTEP diagram depicting the molecular structure of **4** is shown in Figure 4. Relevant bond lengths and angles are given in Table 3, and selected crystal and structure refinement data are shown in Table 2. The guanidinato ligands of complex **4** are fluxional at room temperature, as evidenced by observation (^1H NMR spectroscopy) of a single resonance for the eight isopropyl methyl groups (doublet, 24H) and the four dimethylamino methyl groups (singlet, 12H). Similar spectroscopic features are observed for all $(guan)_2ZrX_2$ derivatives (vide infra).

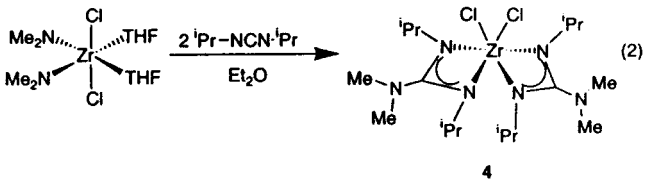

Alkylation of **4** with 2 equiv of MeLi or 2 equiv of $PhCH_2MgCl$ in Et_2O gives $(guan)_2ZrMe_2$ (**5**) and $(guan)_2Zr(CH_2Ph)_2$ (**6**) in 86 and 80% yields, respectively, after recrystallization from pentane (Scheme 2). The isopropyl (methyl and methine) and benzylic (methylene) resonances of **6** are broad in the room-temperature ^1H NMR spectrum, presumably due to hindered rotation of the benzyl and guanidinato ligands. The ^1H NMR spectrum of **6** at 220 K (toluene-d_8) is consistent with a limiting C_2-symmetric structure: four distinct isopropyl methyl resonances, as well as two doublets ($^2J_{HH}$ = 10.0 Hz) for the diastereotopic benzylic protons, are observed. ORTEP diagrams depicting the solid-state structures of **5** and **6** are shown in Figures 5 and 6 along with relevant bond lengths and angles in Tables 4 and 5, respectively. Selected crystal and structure refinement data are given in Tables 2 and 6. The X-ray diffraction data for **6** are consistent with the structural assignment postulated from the low-temperature ^1H NMR spectroscopic data. Additionally, the solid-state structure of **6** reveals that both benzyl ligands adopt undistorted (η^1) coordination modes.

Treatment of **5** with 2 equiv of Me_3SiOTf in benzene produces the bis(triflato) complex $(guan)_2Zr(OTf)_2$ (**7**) in 77% yield along with 2 equiv of Me_4Si (detected by ^1H NMR spectroscopy) (Scheme 2). The isopropyl methyl resonances are broadened in the room-temperature ^1H NMR spectrum of **7**, again presumably due to hindered rotation of the bulky triflato and guanidinato ligands. Crystals of **7** suitable for X-ray diffraction were obtained by allowing the reaction mixture to stand at room temperature overnight. An ORTEP diagram showing the solid-state structure of **7** is presented in Figure 7. Representative bond lengths and angles are given in Table 7; selected crystal and structure refinement data are given in Table 6.

Comments on the Solid-State Structures of Neutral $(guan)_2ZrX_2$ Derivatives (X = Cl, Me, CH_2Ph, OTf). The utility of the guanidinato ligand lies in its ability to stabilize electron-deficient metal centers. Although this effect is likely to be more pronounced in highly electronically unsaturated systems (i.e., metal cations), it is possible that the donor ability of the guanidinato ligand may manifest itself in neutral complexes as well. Analysis of the crystallographic data for $(guan)_2ZrX_2$ (X = Cl, Me, CH_2Ph, OTf) derivatives reveals that the relative electron-withdrawing or -releasing ability of the X ligands affects the degree to which π-donation from the dimethylamino group occurs. Accordingly, **5** and **6**, which bear electron-releasing alkyl ligands and therefore possess more electron-rich metal centers, exhibit Me_2N-C bond lengths of 1.388(3) and 1.385(3) Å (for **5**) and 1.394(4) and 1.385(4) Å (for **6**): slightly shorter than typical C−N single bonds. Complexes **4** and **7**, which bear electron-withdrawing chloride and triflato ligands, have electron-poor metal centers relative to **5** and **6** and, hence, exhibit more contracted Me_2N-C bonds (1.365(5) and 1.360(5) Å for

(33) Chandra, G.; Jenkins, A. D.; Lappert, M. F. *J. Chem. Soc. A* **1970**, 2550.

Table 2. Selected Crystal Data and Data Collection Parameters for Cp(guan)$ZrCl_2$ (1), (guan)$_2ZrCl_2$ (4), and (guan)$_2ZrMe_2$ (5)

	1	4	5
formula	$C_{14}H_{25}N_3Cl_2Zr$	$C_{18}H_{40}Cl_2N_6Zr$	$C_{20}H_{46}N_6Zr$
fw	397.50	502.68	461.84
cryst size (mm)	0.20 × 0.21 × 0.30	0.15 × 0.20 × 0.30	0.10 × 0.20 × 0.30
cryst syst	monoclinic	orthorhombic	triclinic
space group	$P2_1/c$	$Pbca$	$P\bar{1}$
a (Å)	9.4940(2)	15.1279(3)	8.6100(1)
b (Å)	14.3186(4)	16.9122(1)	9.0090(1)
c (Å)	13.0843(4)	20.1017(4)	18.3740(1)
β (deg)	94.735(1)	90.000	94.280(1)
V (Å^3)	1772.62(7)	5142.9(3)	1271.51(3)
Z	4	8	2
d_{calcd} (g/cm^3)	1.489	1.298	1.206
μ(Mo Kα) (cm^{-1})	9.16	6.49	4.47
T (°C)	−159	−103	−99.0
scan type	ω (0.30°/frame)	ω (0.30°/frame)	ω (0.30°/frame)
scan rate (s/frame)	10	10	15
radiation	Mo Kα (λ = 0.710 69 Å)	Mo Kα (λ = 0.710 69 Å)	Mo Kα (λ = 0.710 69 Å)
monochromator	graphite	graphite	graphite
2θ range (deg)	3.0−45.0	3.0−52.3	3.0−45.0
no. of rflns measd	8589 (unique 3281) (R_{int} = 0.025)	27 015 (unique 5583) (R_{int} = 0.044)	6130 (unique 4281) (R_{int} = 0.017)
R	0.029	0.036	0.030
R_w	0.033	0.040	0.036
R_{all}	0.029	0.036	0.030
GOF	2.22	1.36	1.26
p factor	0.030	0.031	0.030
no. of variables	181	244	244

Scheme 1. Salt Metathesis, Disproportionation, and Attempted Quaternization of Cp(guan)$ZrCl_2$ (1)

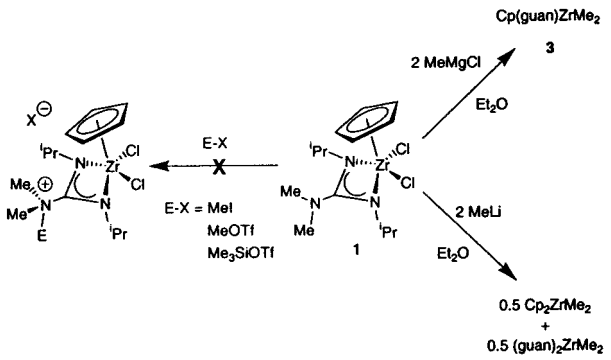

4 and 1.364(3) and 1.356(3) Å for **7**). These data imply that the guanidinato ligand acts as a stronger donor toward the more electron-poor metal centers of complexes **4** and **7**. Consistent with this argument, the mean Zr−N distances of complexes **4** and **7** (2.206 and 2.167 Å, respectively) are slightly but significantly shorter than those of **5** and **6** (2.257 and 2.252 Å, respectively). The angle between the plane of the metal chelate and that of the dimethylamino substituent varies between 39 and 49° for complexes **4**−**7**. While not optimal for delocalization, this does allow for some overlap of the nitrogen p orbital with the π system of the chelate.

Although these effects are subtle, the data suggest that the electronic environment at the metal center dictates the extent of π-donation from the dimethylamino group and, hence, the overall donor strength of the guanidinato ligand. The ligand acts as a more powerful electron donor toward the relatively electron-poor metal centers of complexes **4** and **7** and as a less powerful donor toward the electron-rich metal centers of **5** and **6**.

Methide Abstraction from (guan)$_2ZrMe_2$ (5). A methyl ligand may be abstracted from **5** in a variety of ways to give stable (guan)$_2$Zr(Me)X complexes. Treatment of **5** with 1 equiv of Me_3SiOTf affords (guan)$_2$Zr(Me)OTf (**8**), along with 1 equiv of tetramethylsilane (detected by ^{1}H NMR spectroscopy) (Scheme 3). The triflato ligand of **8** is formulated as inner sphere by virtue of the solubility of the complex in aromatic hydrocarbons and by analogy to other reported early-metal triflato complexes.[34−38] The lower molecular symmetry of **8** compared to that of (guan)$_2ZrX_2$ derivatives

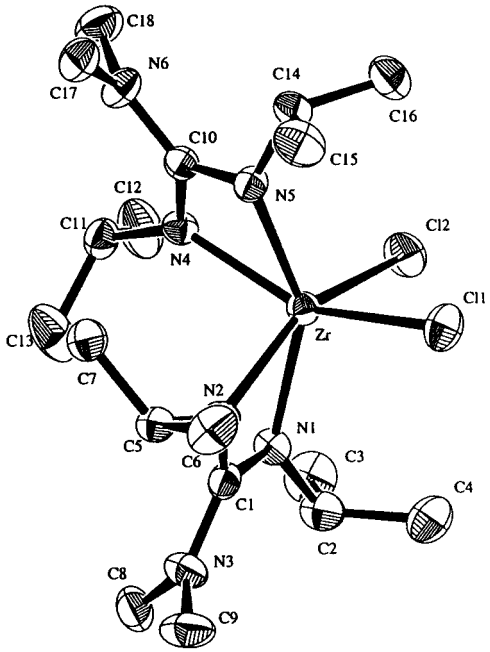

Figure 4. ORTEP diagram of (guan)$_2ZrCl_2$ (**4**) showing atom-numbering scheme (50% thermal ellipsoids). Hydrogen atoms have been omitted for clarity.

(34) Luinstra, G. A. *J. Organomet. Chem.* **1996**, *517*, 209.
(35) Boutonnet, F.; Zablocka, M.; Igau, A.; Marjoral, J.-P.; Jaud, J.; Pietrusiewicz, K. M. *J. Chem. Soc., Chem. Commun.* **1993**, 1487.

Table 3. Metrical Data for (guan)$_2$ZrCl$_2$ (4)

Selected Bond Lengths (Å)			
Zr−Cl(1)	2.441(1)	Zr−Cl(2)	2.446(1)
Zr−N(1)	2.198(3)	Zr−N(4)	2.198(3)
Zr−N(2)	2.218(3)	Zr−N(5)	2.208(3)
N(1)−C(1)	1.362(5)	N(4)−C(10)	1.338(5)
N(2)−C(1)	1.322(5)	N(5)−C(10)	1.360(3)
N(3)−C(1)	1.365(5)	N(6)−C(10)	1.360(5)
Selected Bond Angles (deg)			
N(4)−Zr−N(5)	60.4(1)	Cl(1)−Zr−Cl(2)	91.46(4)
N(1)−Zr−N(2)	60.1(1)	N(1)−C(1)−N(2)	111.0(4)
C(1)−N(3)−C(8)	121.8(4)	N(4)−C(10)−N(5)	110.5(4)
[N(1)−C(1)−N(2)]/ [C(8)−N(3)−C(9)][a]	41.04	[N(4)−C(10)−N(5)]/ [C(17)−N(6)−C(18)][a]	43.57

[a] The angle between the planes of the chelate (N−C−N) and its dimethylamino substituent.

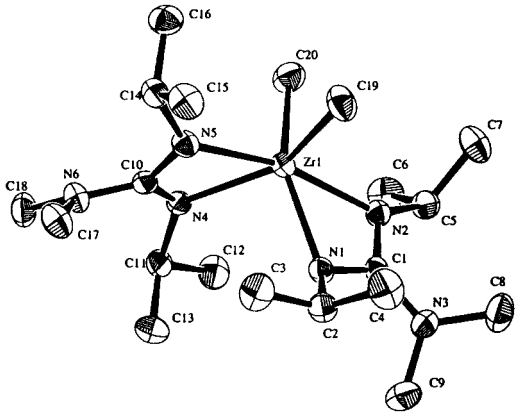

Figure 5. ORTEP diagram of (guan)$_2$ZrMe$_2$ (**5**) showing atom-numbering scheme (50% thermal ellipsoids). Hydrogen atoms have been omitted for clarity.

Scheme 2. Synthesis of (guan)$_2$ZrX$_2$ Derivatives (X = Me (5), CH$_2$Ph (6), OTf (7))

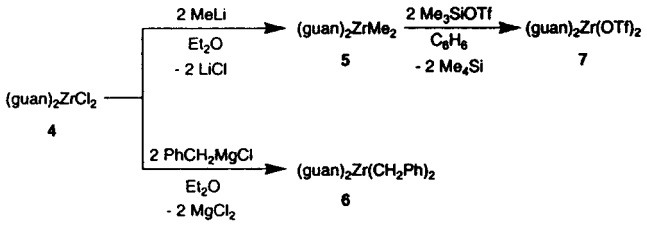

is evident in its ^{1}H NMR spectrum; whereas (guan)$_2$ZrX$_2$ complexes exhibit a single resonance (doublet, 24H) for the eight isopropyl methyl groups on the two guanidinato ligands, the ^{1}H NMR spectrum of **8** contains two resonances (doublets, 12H each) for the same groups.

Reaction of **5** with 1 equiv of tris(pentafluorophenyl)-borane (B(C$_6$F$_5$)$_3$) in pentane results in the formation of [(guan)$_2$ZrMe][MeB(C$_6$F$_5$)$_3$] (**9**) as a pale yellow oil in 96% yield (Scheme 3). Room-temperature ^{1}H NMR analysis of **9** in CD$_2$Cl$_2$ reveals a sharp singlet for the zirconium-bound methyl group (δ 0.86 ppm) and a broad singlet for the boron-bound methyl group (δ 0.47 ppm). These assignments are confirmed by a ^{1}H−^{13}C HMQC experiment, which reveals a ^{13}C resonance at 53 ppm (typical for (guan)$_2$Zr(*C*H$_3$)X (X = Me, OTf, B(C$_6$F$_5$)$_4$) derivatives) correlated to the ^{1}H resonance at 0.86 ppm. Additionally, a broadened ^{13}C resonance at 9.5 ppm correlates to the ^{1}H resonance at 0.47 ppm. The methyl carbon of the MeB(C$_6$F$_5$)$_3$ anion is typically observed to resonate at ≤30 ppm.[13,20,39−41]

Comparison of the ^{19}F NMR spectra of **9** in CD$_2$Cl$_2$ and C$_6$D$_5$Cl reveals only a small difference in the $\Delta(m,p$-F) values between the two solvents. In CD$_2$Cl$_2$ solution, the value of $\Delta(m,p$-F) is 2.4 ppm, whereas in

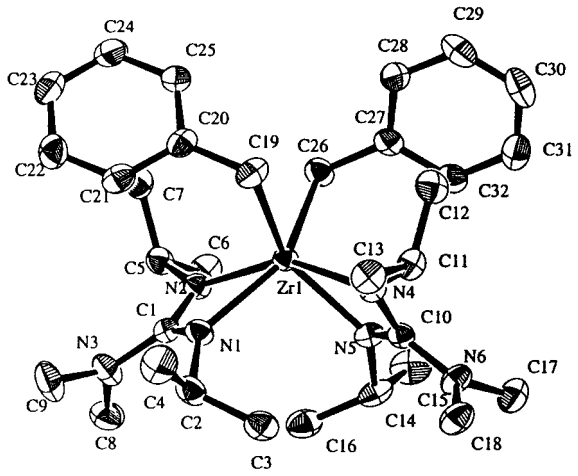

Figure 6. ORTEP diagram of (guan)$_2$Zr(CH$_2$Ph)$_2$ (**6**) showing atom-numbering scheme (50% thermal ellipsoids). Hydrogen atoms have been omitted for clarity.

Table 4. Metrical Data for (guan)$_2$ZrMe$_2$ (5)

Selected Bond Lengths (Å)			
Zr−C(19)	2.267(3)	Zr−C(20)	2.264(3)
Zr−N(1)	2.230(2)	Zr−N(4)	2.249(2)
Zr−N(2)	2.281(2)	Zr−N(5)	2.269(2)
N(1)−C(1)	1.352(3)	N(4)−C(10)	1.338(3)
N(2)−C(1)	1.326(3)	N(5)−C(10)	1.338(3)
N(3)−C(1)	1.385(3)	N(6)−C(10)	1.388(3)
Selected Bond Angles (deg)			
N(1)−Zr−N(2)	58.79(8)	C(19)−Zr−C(20)	92.7(1)
N(4)−Zr−N(5)	58.84(7)	N(1)−C(1)−N(2)	111.6(2)
C(1)−N(3)−C(8)	122.3(2)	N(4)−C(10)−N(5)	112.1(2)
[N(1)−C(1)−N(2)]/ [C(8)−N(3)−C(9)][a]	40.57	[N(4)−C(10)−N(5)]/ [C(17)−N(6)−C(18)][a]	39.36

[a] The angle between the planes of the chelate (N−C−N) and its dimethylamino substituent.

Table 5. Metrical Data for (guan)$_2$Zr(CH$_2$Ph)$_2$ (6)

Selected Bond Lengths (Å)			
Zr−C(19)	2.310(3)	Zr−C(26)	2.323(3)
Zr−N(1)	2.237(2)	Zr−N(4)	2.260(2)
Zr−N(2)	2.271(2)	Zr−N(5)	2.241(2)
N(1)−C(1)	1.335(4)	N(4)−C(10)	1.347(3)
N(2)−C(1)	1.341(4)	N(5)−C(10)	1.344(4)
N(3)−C(1)	1.394(4)	N(6)−C(10)	1.385(4)
Selected Bond Angles (deg)			
N(1)−Zr−N(2)	59.24(9)	N(1)−C(1)−N(2)	112.8(2)
N(4)−Zr−N(5)	59.40(8)	N(4)−C(10)−N(5)	112.0(2)
C(19)−Zr−C(26)	89.7(1)	C(1)−N(3)−C(8)	121.0(3)
Zr−C(19)−C(20)	110.7(2)	Zr−C(26)−C(27)	110.5(2)
[N(1)−C(1)−N(2)]/ [C(8)−N(3)−C(9)][a]	49.46	[N(4)−C(10)−N(5)]/ [C(17)−N(6)−C(18)][a]	43.90

[a] The angle between the planes of the chelate (N−C−N) and its dimethylamino substituent.

(36) Baranger, A. M.; Bergman, R. G. *J. Am. Chem. Soc.* **1994**, *116*, 3822.
(37) Feldman, J.; Calabrese, J. C. *J. Chem. Soc., Chem. Commun.* **1991**, 134.
(38) Roddick, D. M.; Heyn, R. H.; Tilley, T. D. *Organometallics* **1989**, *8*, 324.
(39) Doerrer, L. H.; Green, M. L. H.; Häussinger, D.; Sassmannshausen, J. *J. Chem. Soc., Dalton Trans.* **1999**, 2111.
(40) Gielens, E. E. C. G.; Dijkstra, T. W.; Berno, P.; Meetsma, A.; Hessen, B.; Teuben, J. H. *J. Organomet. Chem.* **1999**, *591*, 88.
(41) Witte, P. T.; Meetsma, A.; Hessen, B. *J. Am. Chem. Soc.* **1997**, *119*, 10561.

Table 6. Selected Crystal and Data Collection Parameters for $(guan)_2Zr(CH_2Ph)_2$ (6), $(guan)_2Zr(OTf)_2$ (7), and $[((guan)_2ZrMe)_2$-μ-Me$][B(C_6F_5)_4]$ (11)

	6	7	11
formula	$C_{32}H_{54}N_6ZrO$	$H_{40}C_{20}ZrS_2O_6F_6N_6$	$C_{72}H_{96.50}Zr_2F_{21.50}N_{12}B$
fw	630.04	729.90	1731.85
cryst size (mm)	0.25 × 0.20 × 0.38	0.30 × 0.15 × 0.27	0.07 × 0.27 × 0.33
cryst syst	monoclinic	monoclinic	monoclinic
space group	$P2_1/c$	$P2_1/n$	$P2_1/c$
a (Å)	11.3795(2)	10.4422(2)	20.6187(3)
b (Å)	17.6096(2)	11.5751(2)	21.7004(2)
c (Å)	18.0488(3)	30.3803(4)	19.7608(4)
β (deg)	95.759(1)	93.692(1)	114.697(1)
V (Å^3)	3598.52(9)	3664.43(9)	8032.9(2)
Z	4	4	4
d_{calcd} (g/cm^3)	1.163	1.323	1.432
μ(Mo Kα) (cm^{-1})	3.36	4.81	30.89
T (°C)	−159	−139	−137
scan type	ω (0.30°/frame)	ω (0.30°/frame)	ω (0.30°/frame)
scan rate (s/frame)	10	10	15
radiation	Mo Kα (λ = 0.710 69 Å)	Mo Kα (λ = 0.710 69 Å)	Mo Kα (λ = 0.710 69 Å)
monochromator	graphite	graphite	graphite
2θ range (deg)	3.0−52.2	3.0−49.4	3.0−49.4
no. of rflns measd	17 209 (unique 6555) (R_{int} = 0.030)	16 382 (unique 6338) (R_{int} = 0.019)	37 506 (unique 13 968) (R_{int} = 0.036)
R	0.029	0.024	0.031
R_w	0.034	0.031	0.034
R_{all}	0.029	0.024	0.061
GOF	1.22	1.21	1.28
p factor	0.031	0.031	0.030
no. of variables	577	424	982

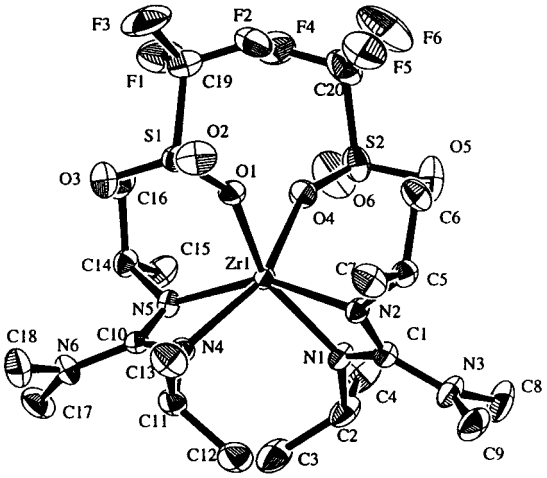

Figure 7. ORTEP diagram of $(guan)_2Zr(OTf)_2$ (**7**) showing atom-numbering scheme (50% thermal ellipsoids). Hydrogen atoms have been omitted for clarity.

Table 7. Metrical Data for $(guan)_2Zr(OTf)_2$ (7)

Selected Bond Lengths (Å)			
Zr−O(1)	2.129(2)	Zr−O(4)	2.124(2)
Zr−N(1)	2.161(2)	Zr−N(4)	2.149(2)
Zr−N(2)	2.168(2)	Zr−N(5)	2.190(2)
N(1)−C(1)	1.348(3)	N(4)−C(10)	1.348(3)
N(2)−C(1)	1.353(3)	N(5)−C(10)	1.354(3)
N(3)−C(1)	1.356(3)	N(6)−C(10)	1.364(3)

Selected Bond Angles (deg)			
N(1)−Zr−N(2)	61.80(7)	N(1)−C(1)−N(2)	110.8(2)
N(4)−Zr−N(5)	61.75(7)	N(4)−C(10)−N(5)	111.0(2)
O(1)−Zr−O(4)	84.66(7)	C(1)−N(3)−C(8)	123.1(3)
[N(1)−C(1)−N(2)]/[C(8)−N(3)−C(9)][a]	37.54	[N(4)−C(10)−N(5)]/[C(17)−N(6)−C(18)][a]	40.34

[a] The angle between the planes of the chelate (N−C−N) and its dimethylamino substituent.

C_6D_5Cl solution, $\Delta(m,p\text{-F})$ is 2.6 ppm. These low (<3 ppm) values of $\Delta(m,p\text{-F})$ imply that the $MeB(C_6F_5)_3$ anion is not strongly associated with the Zr center in these two solvents.[20] The ^{19}F NMR data, coupled with the oily nature of **9** and the observation that **9** is insoluble in aromatic hydrocarbons (benzene, toluene), indicate relatively loose ion pairing between the bis(guanidinato)zirconium methyl cation and the $MeB(C_6F_5)_3$ anion.[12,42] This may be due, in part, to delocalization of positive charge by the guanidinato ligands (as in Figure 2), resulting in a less electrophilic (i.e., "less cationic") metal center and hence weakening cation−anion interactions.

Scheme 3. Methide Abstraction from $(guan)_2ZrMe_2$ (5)

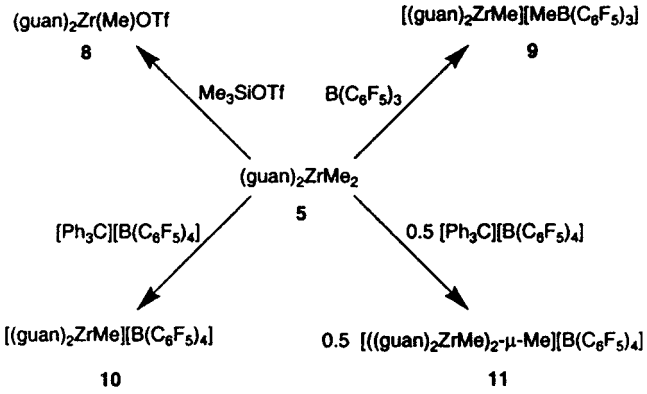

The unique donor ability of the guanidinato ligand allows for isolation and characterization of zirconium methyl cations with the extremely weakly coordinating $B(C_6F_5)_4$ counteranion. Treatment of a pentane solution of **5** with a suspension of $[Ph_3C][B(C_6F_5)_4]$ (1 equiv) in benzene results in the precipitation of a white solid. Removal of the solvent followed by repeated pentane washings gives base-free $[(guan)_2ZrMe][B(C_6F_5)_4]$ (**10**) as a spectroscopically and analytically pure powder in 92% yield (Scheme 3). The thermal stability of **10** is

(42) Sun, Y.; Metz, M. V.; Stern, C. L.; Marks, T. J. *Organometallics* **2000**, *19*, 1625.

unusually high for a zirconium methyl cation with the $B(C_6F_5)_4$ counteranion.[17,20,43,44] While **10** is sensitive to air and moisture, it is stable indefinitely at room temperature under an inert atmosphere and is stable in CH_2Cl_2 solution for several hours. Because of the increased electrophilicity of the cationic metal center, the carbon atom of the methyl ligand of **10** resonates at lower field (δ 51 ppm, chlorobenzene-d_5) than the methyl carbons of the neutral precursor **5** (δ 40 ppm, chlorobenzene-d_5).[13,20] The room-temperature ^{1}H NMR spectrum of complex **10** is similar to those of neutral $(guan)_2ZrX_2$ derivatives. A single sharp resonance (doublet, 24H) is observed for the eight isopropyl methyl groups. Observation of the ^{1}H NMR spectrum of **10** at 188 K (CD_2Cl_2) reveals four inequivalent isopropyl methyl resonances; while dynamic processes involving the guanidinato ligands are slow on the NMR time scale at 188 K, anion and/or solvent coordination to the cationic metal center is still weak and rapid on the NMR time scale at this temperature.

Several workers have observed the formation of cationic methyl-bridged dinuclear complexes under varied reaction conditions.[7,11,20,45−51] Complexes of this type have been implicated as inactive components in some polymerization experiments.[7] Treatment of **5** with 0.5 equiv of $[Ph_3C][B(C_6F_5)_4]$ in pentane/benzene solution results in the precipitation of the dinuclear cation $[((guan)_2ZrMe)_2$-μ-$Me][B(C_6F_5)_4]$ (**11**) as a white powder (Scheme 3). Alternatively, **11** may be generated and observed upon mixing equimolar amounts of **5** and **10** at room temperature in chlorobenzene-d_5 solution. This indicates that neutral **5** is a better ligand for the cationic zirconium center than either the weakly coordinating $B(C_6F_5)_4$ anion or the chlorinated solvent.[47]

The room-temperature ^{1}H NMR spectrum of **11** shows a single sharp resonance for the nine methyl protons of the complex, indicating that bridge−terminal methyl group exchange is fast on the NMR time scale. Decoalescence of the bridging and terminal methyl groups is observed by ^{1}H NMR spectroscopy at 224.0 K in CD_2Cl_2. In the low-temperature limit (188 K) bridge−terminal exchange is slow on the NMR time scale and sharp resonances corresponding to the two methyl environments are observed. The resonance assigned to the two terminal methyl groups (δ 0.33 ppm) can be integrated and is found to correspond to six protons. The bridging methyl resonance (δ 1.11 ppm) cannot be accurately integrated, due to overlap with the multiple isopropyl methyl resonances observed at 188 K. However, the peak is assigned as a Zr-bound methyl group by a ^{1}H−^{13}C HMQC experiment, which shows that the resonance at 1.11 ppm in the ^{1}H spectrum correlates to a ^{13}C resonance at δ 46 ppm. The ^{13}C shift of δ 46 ppm falls into the observed range for $(guan)_2Zr(CH_3)X$ complexes (X = Me, OTf, $MeB(C_6F_5)_3$, $B(C_6F_5)_4$).

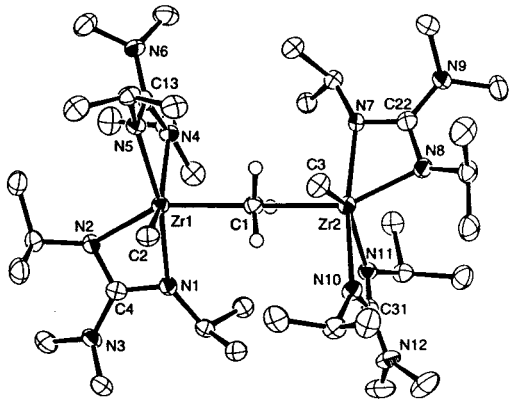

Figure 8. ORTEP diagram showing the cationic portion of $[((guan)_2ZrMe)_2$-μ-$Me][B(C_6F_5)_4]$ (**11**) with atom-numbering scheme (50% thermal ellipsoids). Hydrogen atoms on the bridging methyl group are shown in their refined positions. All other hydrogen atoms have been omitted for clarity.

Crystals of **11** suitable for X-ray diffraction were grown from a concentrated fluorobenzene solution at −30 °C. An ORTEP diagram of **11** is shown in Figure 8, with relevant bond lengths and angles given in Table 8. Selected crystal and structure refinement data are shown in Table 6. Dinuclear cation **11** crystallizes with 1.5 equiv of fluorobenzene in the crystal lattice. The crystal structure revealed no close contacts between the cation and the anion or fluorobenzene. The solid-state structure of **11** is interesting in several respects. The two terminal methyl groups are staggered by 33.0° with respect to one another; similar arrangements have been observed by Marks and co-workers[11] and by Schrock and co-workers.[51] The Zr−CH_3−Zr bridge of **11** is nearly linear (170.84(13)°), but the two Zr−C bond lengths of the bridge are significantly different (Zr(1)−C(1) = 2.397(3) Å; Zr(2)−C(1) = 2.489(3) Å). The hydrogens on the bridging methyl group were located and are directed toward the longer Zr−C bond (sum of angles around C(1) 351.0°). Apart from the distinct Zr−$C_{bridging}$ bond lengths, there are no significant differences between the two sides of the cationic portion of **11**. The Me_2N−C bond lengths of **11** vary between 1.362(4) and 1.382(4) Å, in the same range observed for the $(guan)_2ZrX_2$ derivatives. The angles between the four metal chelates of **11** and the dimethylamino groups attached to them range from 36 to 45°.

Benzyl Anion Abstraction from 6. In analogy to the synthesis of the methyl cations, treatment of **6** with $[Ph_3C][B(C_6F_5)_4]$ in CH_2Cl_2 affords $[(guan)_2Zr(CH_2Ph)]$-$[B(C_6F_5)_4]$ (**15**) as an analytically pure pale yellow powder in 91% yield (eq 3). Several workers have

$$\underset{\textbf{6}}{(guan)_2Zr(CH_2Ph)_2} \xrightarrow[CH_2Cl_2]{[Ph_3C][B(C_6F_5)_4]} \underset{\textbf{15}}{[(guan)_2ZrCH_2Ph][B(C_6F_5)_4]} \quad (3)$$
$$\text{- } Ph_3CCH_2Ph$$

reported zirconium benzyl cations with weakly coordi-

(43) Baumann, R.; Davis, W. M.; Schrock, R. R. *J. Am. Chem. Soc.* **1997**, *119*, 3830.
(44) Schrock, R. R.; Liang, L. C.; Baumann, R.; Davis, W. R. *J. Organomet. Chem.* **1999**, *591*, 163.
(45) Yang, X.; Stern, C. L.; Marks, T. J. *Organometallics* **1991**, *10*, 840.
(46) Beck, S.; Prosenc, M. H.; Brintzinger, H. H.; Goretzki, R.; Herfert, N.; Fink, G. *J. Mol. Catal. A* **1996**, *111*, 67.
(47) Bochmann, M.; Lancaster, S. J. *Angew. Chem., Int. Ed. Engl.* **1994**, *33*, 1634.
(48) Wang, Q.; Gillis, D. J.; Quyoum, R.; Jeremic, D.; Tudoret, M. J.; Baird, M. C. *J. Organomet. Chem.* **1997**, *527*, 7.
(49) Köhler, K.; Piers, W. E.; Jarvis, A. P.; Xin, S.; Feng, Y.; Bravakis, A. M.; Collins, S.; Clegg, W.; Yap, G. P. A.; Marder, T. B. *Organometallics* **1998**, *17*, 3557.
(50) Williams, V. C.; Dai, C.; Li, Z.; Collins, S.; Piers, W. E.; Clegg, W.; Elsegood, M. R. J.; Marder, T. B. *Angew. Chem., Int. Ed.* **1999**, *38*, 3695.
(51) Schrock, R. R.; Casado, A. L.; Goodman, J. T.; Liang, L.-C.; Bonitatebus, P. J.; Davis, W. M. *Organometallics* **2000**, *19*, 5325.

Table 8. Metrical Data for [(guan)$_2$ZrMe)$_2$-μ-Me][B(C$_6$F$_5$)$_4$] (11)

Selected Bond Lengths (Å)			
Zr(1)−C(1)	2.397(3)	Zr(1)−C(2)	2.258(3)
Zr(2)−C(1)	2.489(3)	Zr(2)−C(3)	2.251(3)
Zr(1)−N(1)	2.234(2)	Zr(1)−N(4)	2.205(2)
Zr(1)−N(2)	2.196(2)	Zr(1)−N(5)	2.248(2)
Zr(2)−N(7)	2.260(2)	Zr(2)−N(10)	2.241(2)
Zr(2)−N(8)	2.147(2)	Zr(2)−N(11)	2.226(2)
N(1)−C(4)	1.329(4)	N(4)−C(13)	1.348(4)
N(2)−C(4)	1.350(4)	N(5)−C(13)	1.346(4)
N(3)−C(4)	1.382(4)	N(6)−C(13)	1.362(4)
N(7)−C(22)	1.336(4)	N(10)−C(31)	1.343(4)
N(8)−C(22)	1.358(4)	N(11)−C(31)	1.343(4)
N(9)−C(22)	1.372(4)	N(12)−C(31)	1.363(4)

Selected Bond Angles (deg)			
C(1)−Zr(1)−C(2)	88.48(10)	Zr(1)−C(1)−Zr(2)	170.84(13)
C(1)−Zr(2)−C(3)	90.11(11)	N(1)−Zr(1)−N(2)	60.07(9)
N(7)−Zr(2)−N(8)	60.74(9)	N(4)−Zr(1)−N(5)	59.69(8)
N(10)−Zr(2)−N(11)	59.42(8)	N(1)−C(4)−N(2)	111.8(3)
N(7)−C(22)−N(8)	111.7(3)	N(4)−C(13)−N(4)	110.7(3)
N(10)−C(31)−N(11)	111.1(3)	[N(1)−C(4)−N(2)]/[C(11)−N(3)−C(12)][a]	46.45
[N(4)−C(13)−N(5)]/[C(20)−N(6)−C(21)][a]	36.67	[N(7)−C(22)−N(8)]/[C(29)−N(9)−C(30)][a]	39.95
[N(10)−C(31)−N(11)]/[C(38)−N(12)−C(39)][a]	41.16		

[a] The angle between the planes of the chelate (N−C−N) and its dimethylamino substituent.

nating anions.[9,20,52−60] A common feature of these compounds both in solution and in the solid state is a strong interaction of the ipso carbon of the aryl ring with the cationic metal center, resulting in a distorted, η^2-coordinated benzyl ligand. Spectroscopically, η^2-benzyl ligands typically exhibit high (>130 Hz) benzylic $^1J_{CH}$ coupling constants and upfield-shifted ortho ^{1}H resonances.[9,20,58,61−63] The spectroscopic data for **15** suggest that the benzyl ligand adopts an undistorted (η^1) coordination mode. Evidence for this comes from the small benzylic $^1J_{CH}$ coupling constant (127 Hz in CD_2Cl_2; 125 Hz in chlorobenzene-d_5), which is only slightly higher than the coupling constant measured for the neutral dibenzyl derivative **6** ($^1J_{CH}$ = 123 Hz) which bears undistorted benzyl ligands, as shown by X-ray diffraction (vide supra). Although the ortho protons of the benzyl ligand could not be assigned, due to overlap with the solvent (C_6D_5Cl), all aryl protons of **15** resonate at ≥6.9 ppm, the expected range for an undistorted benzyl ligand.[61] Despite numerous attempts, crystals of **15** suitable for an X-ray diffraction study could not be obtained. Monodentate coordination of a benzyl ligand to a base-free cationic zirconium center is rare;[64] it is possible that the guanidinato ligand stabilizes the electron-deficient metal center such that coordination to the π-system of the aryl ring is unnecessary.

Table 9. Polymerization Data for Complexes 4, 5, and 10

run	catal	cocatal[a]	T (°C)	[C_2H_4][b]	[Zr][c]	amt of polym[d]	M_w/M_n	activity[e]
1	std[f]	MMAO[g,h]	75	106	1.0	52.3	3.2	98 308
2	**4**	MMAO[h]	75	106	2.0	2.5	24.8[i]	2350
3	**4**	MMAO[j]	75	106	14.1	1.2	36.7[i]	160
4	**5**	[Ph_3C]-[B(C_6F_5)$_4$]	55	85	21.6	1.1	49.7[i]	120
5	**10**	none	85	130	4.4	0.4	nd[l]	103
6	**10**	none	50	130	8.9	0.9	nd	116
7	**10**	none	50	130	13.3	0.2	nd	17
8[k]	**10**	none	75	85	13.3	2.0	nd	354

[a] 100−200 μmol of triisobutylaluminum (TIBA) was used in all the runs as a scrubbing agent. [b] In units of psi. [c] In units of μmol. [d] In units of g. [e] Activity = g of polymer (mmol of cat)$^{-1}$ (100 psi of C_2H_4)$^{-1}$ h^{-1}. [f] The standard used was (^{n}BuCp)$_2$ZrCl_2. [g] MMAO = modified methylaluminoxane. [h] [Al]:[Zr] = 500. [i] Polymer from these runs showed broad and/or bimodal molecular weight distributions. See the Supporting Information for a representative GPC trace. [j] [Al]:[Zr] = 355. [k] All runs except run 8 were carried out with 10% 1-hexene comonomer. [l] nd = not determined.

Olefin Polymerization Experiments. Neutral bis(guanidinato)zirconium complexes **4** and **5** and alkyl salt **10** were screened for ethylene homopolymerization and ethylene/1-hexene copolymerization. Results of the polymerization experiments are shown in Table 9. All of the compounds investigated are 1−3 orders of magnitude less active than (^{n}BuCp)$_2$ZrCl_2. This is not surprising in light of the very modest ethylene polymerization activities reported for structurally related[3] bis(amidinato)zirconium complexes.[65−69] Differential scanning calorimetry and size-exclusion chromatography assays on the polymer obtained in runs 2−4 revealed broad

(52) Martin, A.; Uhrhammer, R.; Gardner, T. G.; Jordan, R. F.; Rogers, R. D. *Organometallics* **1998**, *17*, 382.
(53) Tsukahara, T.; Swenson, D. C.; Jordan, R. F. *Organometallics* **1997**, *16*, 3303.
(54) Black, D. G.; Swenson, D. C.; Jordan, R. F.; Rogers, R. D. *Organometallics* **1995**, *14*, 3539.
(55) Borkowsky, S. L.; Baenziger, N. C.; Jordan, R. F. *Organometallics* **1993**, *12*, 486.
(56) Crowther, D. J.; Borkowsky, S. L.; Swenson, D. C.; Meyer, T. Y.; Jordan, R. F. *Organometallics* **1993**, *12*, 2897.
(57) Bochmann, M.; Lancaster, S. J.; Hursthouse, M. B.; Abdul Malik, K. M. *Organometallics* **1994**, *13*, 2235.
(58) Pellecchia, C.; Immirzi, A.; Grassi, A.; Zambelli, A. *Organometallics* **1993**, *12*, 4473.
(59) Uhrhammer, R.; Black, D. G.; Gardner, T. G.; Olsen, J. D.; Jordan, R. F. *J. Am. Chem. Soc.* **1993**, *115*, 8493.
(60) Bochmann, M.; Lancaster, S. J. *Organometallics* **1993**, *12*, 633.
(61) Latesky, S. L.; McMullen, A. K.; Niccolai, G. P.; Rothwell, I. P.; Huffman, J. C. *Organometallics* **1985**, *4*, 902.
(62) Mintz, E. A.; Moloy, K. G.; Marks, T. J.; Day, V. W. *J. Am. Chem. Soc.* **1982**, *104*, 4692.
(63) Giesbrecht, G. R.; Whitener, G. D.; Arnold, J. *Organometallics* **2000**, *19*, 2809.
(64) Thorn, M. G.; Etheridge, Z. C.; Fanwick, P. E.; Rothwell, I. P. *J. Organomet. Chem.* **1999**, *591*, 148.
(65) Littke, A.; Sleiman, N.; Bensimon, C.; Richeson, D. S.; Yap, G. P. A.; Brown, S. J. *Organometallics* **1998**, *17*, 446.
(66) Hagadorn, J. R.; Arnold, J. *J. Chem. Soc., Dalton Trans.* **1997**, 3087.
(67) Walther, D.; Fischer, R.; Gorls, H.; Koch, J.; Schweder, B. *J. Organomet. Chem.* **1996**, *508*, 13.
(68) Flores, J. C.; Chien, J. C. W.; Rausch, M. D. *Organometallics* **1995**, *14*, 1827.
(69) Herskovics-Korine, D.; Eisen, M. S. *J. Organomet. Chem.* **1995**, *503*, 307.

and/or bimodal molecular weight distributions (see Supporting Information). This is due, possibly, to abstraction of one or both of the guanidinato ligands by excess aluminum present (as MMAO or triisobutylaluminum (TIBA)) to generate multiple active species.[70] Analysis of the polymer obtained in runs 4 and 8 by $^{13}C\{^1H\}$ NMR spectroscopy revealed a preponderance of saturated end groups, indicating that the dominant mode of chain termination is chain transfer to aluminum.[71] The $^{13}C\{^1H\}$ NMR spectrum of the ethylene/1-hexene copolymer obtained in run 4 indicated low 1-hexene incorporation into the polymer (4.56 ± 0.53 butyl branches per 1000 carbons).[72,73]

The observed polymerization activities appear to be sensitive to temperature, pressure, and catalyst concentration. For example, a 7-fold increase in the concentration of **4** resulted in a drop in activity of over an order of magnitude (runs 2 and 3) at 75 °C and 106 psi of C_2H_4. Simultaneously lowering the reactor temperature from 85 to 50 °C and doubling the catalyst concentration from 4.4 to 8.9 μmol had little effect on the activity of **10** (runs 5 and 6), but a further increase in catalyst concentration to 13.3 μmol caused a substantial decrease in activity (run 7) at 50 °C. The attenuated activities observed at high concentrations of **4** and **10** (runs 3 and 7) are consistent with previous reports that low zirconium concentrations lead to higher polymerization activities, due to the suppression of bimolecular deactivation pathways.[70] Run 8 was performed in the absence of 1-hexene and showed the highest activity of any of the **10**-derived catalysts, indicating possible inhibition of the polymerization by the α-olefin.[71] Conversion of the activity figures for the two most active catalysts (runs 2 and 8) to the units proposed by Gibson[4] gives activities of 342 and 53 g of polymer (mmol of Zr)$^{-1}$ h^{-1} bar^{-1}, respectively. According to Gibson's classification,[4] complex **4** therefore rates as "highly" active under these conditions (run 2), whereas complex **10** is "moderately" active (run 8). Activation of **5** with $B(C_6F_5)_3$ under several sets of conditions failed to yield an active polymerization catalyst. Recent work by Marks,[74,75] Brintzinger,[76] and Ziegler[77] has shown that the $MeB(C_6F_5)_3$ anion may interact quite strongly with cationic zirconium centers, especially in nonpolar media.[74,75,77] Given that these polymerization experiments were carried out in hexanes, it is likely that the $MeB(C_6F_5)_3$ anions resulting from activation by $B(C_6F_5)_3$ were associated sufficiently strongly with the metal to shut down polymerization completely.

Given the broad, bimodal molecular weight distributions observed in the polymerization experiments, care must be taken in the interpretation of the above data; it is clearly unwise to form conclusions about the nature of the active catalyst(s) in these experiments. It is likely that, although the guanidinato ligand resisted electrophilic attack under stoichiometric conditions, the large excess of Lewis acid present in the reactor (as MMAO and/or TIBA) resulted in complex degradation via ligand abstraction. Current work in this area is focused on the interaction of bis(guanidinato)alkylzirconium cations with olefins in the absence of aluminum-containing additives.

Summary and Conclusions

We have shown that a variety of neutral and cationic alkylzirconium complexes bearing guanidinato ancillary ligands can be synthesized and isolated. Reactivity and structural investigations have shown that π-donation from the dimethylamino moiety of the guanidinato ligand plays an important role in the chemistry of these complexes. Most notable is the thermal stability of the bis(guanidinato)methylzirconium cation when paired with the extremely weakly coordinating tetrakis(pentafluorophenyl)borate anion. We ascribe this stability to the ability of the guanidinato ligands to act as strong electron donors toward the cationic metal center, thereby delocalizing the positive charge into the ligand framework. The bis(guanidinato)benzylzirconium cation exhibits (by ^{13}C and ^1H NMR spectroscopy) unusual η^1 coordination of the benzyl ligand to the cationic zirconium center. Although the bis(guanidinato)zirconium complexes screened showed low to modest ethylene polymerization activity, it is hoped that the stability of the alkylzirconium cations responsible for the polymerization will permit detailed studies on the interactions between the cationic metal center and olefin units.

Experimental Section

General Procedures. Unless otherwise noted, reactions and manipulations were performed at ambient temperature in an inert-atmosphere (N_2) glovebox or using standard Schlenk and high-vacuum-line techniques. Glassware was dried overnight at 150 °C or flame-dried immediately prior to use. All NMR spectra were obtained at ambient temperature (except when noted) using Bruker AMX-300, AMX-400, or DRX-500 spectrometers. ^1H NMR chemical shifts (δ) are reported in parts per million (ppm) relative to residual protiated solvent. $^{13}C\{^1H\}$ NMR chemical shifts (δ) are reported in ppm relative to the carbon resonance of the deuterated solvent. ^{19}F chemical shifts (δ) are reported relative to external $CFCl_3$ (0.00). ^{11}B chemical shifts (δ) are reported relative to external $BF_3{\cdot}OEt_2$ in C_6D_6 (0.00). In cases where assignment of $^{13}C\{^1H\}$ resonances was ambiguous, standard DEPT 45, 90, and/or 135° pulse sequences were utilized. Unless otherwise noted, infrared (IR) spectra were recorded as Nujol mulls between NaCl plates. Elemental analyses were performed at the University of California, Berkeley Microanalytical Facility on a Perkin-Elmer 2400 Series II CHNO/S analyzer.

Materials. Unless otherwise noted, reagents were purchased from commercial suppliers and used without further purification. Pentane, hexanes, benzene, and toluene (Fisher) were passed through a column of activated alumina (type A2, size 12 × 32, Purifry Co.) under nitrogen pressure and sparged with N_2 prior to use. Diethyl ether and tetrahydrofuran (Fisher) were distilled from purple sodium/benzophenone ketyl under N_2 prior to use. Deuterated solvents (Cambridge Isotope Laboratories) were purified by vacuum transfer from the

(70) Brintzinger, H. H.; Fischer, D.; Mülhaupt, R.; Rieger, R.; Waymouth, R. M. *Angew. Chem., Int. Ed. Engl.* **1995**, *34*, 1143.
(71) Janiak, C. In *Metallocenes: Synthesis, Reactivity, and Applications*; Togni, A., Halterman, R. L., Eds.; Wiley-VCH: New York, 1998; Vol. 2, p 547.
(72) Soga, K.; Uozumi, T.; Nakamura, S.; Toneri, T.; Teranishi, T.; Sano, T.; Arai, T. *Macromol. Chem. Phys.* **1996**, *197*, 4237.
(73) McKnight, A. L.; Waymouth, R. M. *Chem. Rev.* **1998**, *98*, 2587.
(74) Beswick, C. L.; Marks, T. J. *J. Am. Chem. Soc.* **2000**, *122*, 10358.
(75) Deck, P. A.; Beswick, C. L.; Marks, T. J. *J. Am. Chem. Soc.* **1998**, *120*, 1772.
(76) Beck, S.; Lieber, S.; Schaper, F.; Geyer, A.; Brintzinger, H. H. *J. Am. Chem. Soc.* **2001**, *123*, 1483.
(77) Vanka, K.; Chan, M. S. W.; Pye, C. C.; Ziegler, T. *Organometallics* **2000**, *19*, 1841.

appropriate drying agent (Na/Ph_2CO or CaH_2) prior to use. Diisopropylcarbodiimide (Lancaster) was distilled from CaH_2 and degassed prior to use. $ZrCl_4$ and $Zr(NMe_2)_4$ were sublimed prior to use. $(Me_2N)_2ZrCl_2(THF)_2$ was prepared according to a literature procedure.[78]

Cp(guan)ZrCl$_2$ (1). A 250 mL Schlenk tube was charged with $LiNMe_2$ (0.251 g, 4.9 mmol) and 100 mL of Et_2O. The resulting colorless suspension was cooled to 0 °C, at which temperature diisopropylcarbodiimide (0.83 mL, 5.4 mmol) was added dropwise via syringe. The reaction mixture was warmed to room temperature over 2 h. The resulting cloudy solution of lithium guanidinate reagent **2** was cannula-transferred into a 250 mL Schlenk tube containing a solution of $CpZrCl_3$ (1.291 g, 4.91 mmol) in THF (100 mL) at −78 °C. The reaction mixture was stirred for 20 min at −78 °C and was warmed to room temperature overnight. Removal of solvent in vacuo, followed by extraction into Et_2O (200 mL) and filtration, gave a clear, yellow solution. Et_2O was removed in vacuo to give crude **1** as a yellow powder. Recrystallization from toluene at −78 °C gave pure **1** as yellow-orange crystals (1.31 g, 67%). ^{1}H NMR (500 MHz, C_6D_6): δ 6.40 (s, 5H, C_5H_5), 3.40 (sept, 2H, C*H*$(CH_3)_2$, J = 6.5 Hz), 2.13 (s, 6H, N(C*H*$_3)_2$), 1.17 (d, 12H, CH(C*H*$_3)_2$, J = 6.5 Hz) ppm. ^{13}C{^{1}H} NMR (125 MHz, C_6D_6): δ 170.1 (s, N$_3$*C*), 115.8 (s, *C*$_5$H$_5$), 48.6 (s, *C*H$(CH_3)_2$), 40.2 (s, N(*C*H$_3)_2$), 24.2 (s, CH(*C*H$_3)_2$) ppm. FT-IR: 1625 (w), 1522 (m), 1341 (m), 1198 (m), 1126 (m), 1058 (m), 1018 (m), 837 (m), 815 (s), 750 (w) cm^{-1}. Anal. Calcd for $ZrC_{14}H_{25}N_3Cl_2$: C, 42.30; H, 6.34; N, 10.57. Found: C, 42.60; H, 6.11; N, 10.36.

Cp(guan)ZrMe$_2$ (3). A 250 mL Schlenk tube was charged with **1** (0.407 g, 1.02 mmol), and Et_2O (40 mL). The resulting yellow suspension was cooled to −78 °C. At this temperature, a MeMgCl solution (0. 72 mL, 3.0 M in THF, 2.15 mmol) was added dropwise via syringe. The reaction mixture was stirred at −78 °C for 30 min and was then warmed to room temperature over 11 h. Removal of solvent under reduced pressure, followed by extraction into pentane (2 × 25 mL) and filtration, gave a clear, colorless solution. Concentration of this solution to approximately 10 mL followed by cooling to −30 °C gave pure **3** as colorless crystals (0.224 g, 61%). ^{1}H NMR (300 MHz, C_6D_6): δ 6.29 (s, 5H, C_5H_5), 3.41 (sept, 2H, C*H*$(CH_3)_2$, J = 6.5 Hz), 2.33 (s, 6H, N(C*H*$_3)_2$), 1.03 (d, 12H, CH(C*H*$_3)_2$, J = 6.5 Hz), 0.52 (s, 6H, Zr(C*H*$_3)_2$) ppm. ^{13}C{^{1}H} NMR (125 MHz, C_6D_6): δ 172.9 (s, N$_3$*C*), 111.5 (s, *C*$_5$H$_5$), 47.0 (s, *C*H$(CH_3)_2$), 42.7 (s, Zr(*C*H$_3)_2$), 39.7 (s, N(*C*H$_3)_2$), 24.4 (s, CH(*C*H$_3)_2$) ppm. FT-IR: 1619 (w), 1514 (s), 1404 (s), 1375 (s), 1193 (s), 1170 (m), 1122 (s), 1054 (s), 1015 (m), 936 (w), 798 (s), 746 (m), 704 (w) cm^{-1}. Anal. Calcd for $ZrC_{16}H_{31}N_3$: C, 53.88; H, 8.76; N, 11.78. Found: C, 53.67; H, 8.63; N, 11.69.

(guan)$_2$ZrCl$_2$ (4). A 100 mL round-bottomed flask was charged with $(Me_2N)_2ZrCl_2(THF)_2$ (0.738 g, 1.98 mmol) and Et_2O (50 mL). The resulting pale yellow solution was cooled to −20 °C, and diisopropylcarbodiimide (0.70 mL, 4.5 mmol) was added via syringe. The reaction mixture was warmed to room temperature overnight. The pale yellow solution was concentrated until crystals formed and then cooled to −30 °C overnight. Pale yellow crystals were isolated by filtration (0.540 g, two crops, 54%). ^{1}H NMR (C_6D_6, 500 MHz): 3.56 (septet, J = 6.5 Hz, 4H, C*H*$(CH_3)_2$), 2.33 (s, 12 H, N(C*H*$_3)_2$), 1.44 (d, J = 6.4 Hz, 24H, CH(C*H*$_3)_2$). ^{13}C{^{1}H} NMR (C_6D_6, 500 MHz): 173.4 (s, N$_3$*C*), 48.0 (s, NCH$(CH_3)_2$), 40.0 (s, N(*C*H$_3)_2$), 25.1 (s, NCH(*C*H$_3)_2$). FT-IR: 1620 (m), 1531 (m), 1455 (m), 1404 (m), 1378 (m), 1348 (m), 1318 (w), 1275 (w), 1191 (m), 1128 (w), 1059 (m), 936 (w), 743 (w), 703 (w), 541 (w) cm^{-1}. Anal. Calcd for $C_{18}H_{40}N_6Cl_2Zr$: C, 43.01; H, 8.02; N, 16.72. Found C, 43.07; H, 8.29; N, 16.39.

(guan)$_2$ZrMe$_2$ (5). A 1 L Schlenk tube was charged with **4** (7.17 g, 14 mmol) and Et_2O (400 mL). The resulting colorless suspension was cooled to −60 °C. At this temperature, a solution of MeLi (22 mL, 1.4 M in Et_2O, 31 mmol) was added dropwise over 8 min via syringe. The reaction mixture was stirred at −60 °C for 45 min and was then warmed to room temperature over 3.5 h. Removal of the solvent under reduced pressure and extraction into pentane (2 × 50 mL) followed by filtration gave a clear, pale yellow solution. Concentration of this solution to approximately 30 mL followed by cooling to −78 °C for 2 days gave colorless crystals of **5** (5.73 g, 86%). ^{1}H NMR (300 MHz, C_6D_6): δ 3.68 (sept, 4H, C*H*$(CH_3)_2$ J = 6.5 Hz), 2.44 (s, 12H, N(C*H*$_3)_2$), 1.36 (d, 24H, CH(C*H*$_3)_2$, J = 6.5 Hz), 0.95 (s, 6H, ZrC*H*$_3$) ppm. ^{13}C{^{1}H} NMR (125 MHz, C_6D_6): δ 174.3 (s, N$_3$*C*), 47.6 (s, *C*H$(CH_3)_2$), 42.9 (s, Zr*C*H$_3$), 40.2 (s, N(*C*H$_3)_2$), 25.4 (s, CH(*C*H$_3)_2$). FT-IR: 2614 (w), 1639 (w), 1515 (s), 1454 (s), 1279 (m), 1187 (s), 1122 (s), 1055 (s), 938 (w), 875 (w), 831 (w), 743 (s), 709 (m) cm^{-1}. Anal. Calcd for $ZrC_{20}H_{46}N_6$: C, 52.01; H, 10.04; N, 18.20. Found: C, 52.20; H, 10.10; N, 18.11.

(guan)$_2$Zr(CH$_2$Ph)$_2$ (6). A 500 mL Schlenk tube was charged with **4** (2.11 g, 4.2 mmol) and Et_2O (200 mL). The resulting colorless suspension was cooled to −78 °C. At this temperature, a solution of benzylmagnesium chloride (8.8 mL, 1.0 M in Et_2O, 8.8 mmol) was added dropwise via syringe. The resulting yellow heterogeneous reaction mixture was warmed to room temperature with stirring over 15 h. Removal of solvent under reduced pressure and extraction into pentane (3 × 70 mL) followed by filtration gave a clear, bright yellow solution. Concentration of this solution to approximately 40 mL, followed by storage at −30 °C overnight, gave yellow needles of pure **6** (2.10 g, 80%). ^{1}H NMR (500 MHz, C_6D_6, 300 K): δ 7.46 (d, 4 H, Ar *o-H*, J = 7.5 Hz), 7.24 (t, 4H, Ar *m-H*, J = 7.5 Hz), 6.95 (t, 2H, Ar *p-H*, J = 7.5 Hz), 3.54 (s (br), 4H, C*H*$(CH_3)_2$), 2.76 (s (br), 2H, Zr(C*H*$_2$Ph)$_2$), 2.40 (s, 12H, N(C*H*$_3)_2$), 1.12 ppm (s (br), 24H, CH(C*H*$_3)_2$) ppm. ^{1}H NMR (500 MHz, C_7D_8, 220 K) 7.57 (d, 4H, Ar *o-H*, J = 7.5 Hz), 7.32 (t, 4H, Ar *m-H*, J = 7.5 Hz), 3.51 (sept, 2H, C*H*$(CH_3)_2$, J = 6.5 Hz), 3.44 (sept, 2H, C*H*$(CH_3)_2$, J = 6.5 Hz), 3.01 (d, 2H, Zr(C*H*$_2$Ph)$_2$, J = 10.0 Hz), 2.69 (d, 2H, Zr(C*H*$_2$Ph)$_2$, J = 10.0 Hz), 2.38 (s, 6H, N(C*H*$_3)_2$), 2.28 (s, 6H, N(C*H*$_3)_2$), 1.36 (d, 6H, CH(C*H*$_3)_2$, J = 6.0 Hz), 1.33 (d, 6H, CH(C*H*$_3)_2$, J = 6.5 Hz), 1.03 (d, 6H, CH-(C*H*$_3)_2$, J = 6.5 Hz), 0.77 (d, 6H, CH(C*H*$_3)_2$, J = 6.5 Hz) ppm (para proton resonance of benzyl ligands could not be resolved due to overlap with the solvent). ^{13}C{^{1}H} NMR (125 MHz, C_6D_6): δ 175.3 (s, N$_3$*C*), 149.9 (s, *p*-*C*$_6$H$_5$), 128.6 (s, *m*-*C*$_6$H$_5$), 120.7 (s, *o*-*C*$_6$H$_5$), 72.5 (s, Zr*C*H$_2$Ph), 48.2 (s (br), *C*H$(CH_3)_2$), 40.0 (s, N(*C*H$_3)_2$), 25.2 (s (br), CH(*C*H$_3)_2$) ppm (ipso carbon resonance of benzyl ligands was not detected). FT-IR: 1592 (m), 1514 (m), 1402 (s), 1186 (m), 1137 (w), 1054 (m), 956 (m), 875 (w), 793 (w), 744 (m), 695 (m) cm^{-1}. Anal. Calcd for $C_{32}H_{54}$-$(C_5H_{12})_{0.5}ZrN_6$ (complex **6** passed analysis with exactly 0.5 equiv of pentane included in the crystal lattice, as was confirmed by ^{1}H NMR analysis of the analytical sample): C, 63.74; H, 9.30; N, 12.93. Found: C, 63.81; H, 9.31; N, 12.92.

(guan)$_2$Zr(OTf)$_2$ (7). A 200 mL Schlenk tube was charged with **5** (0.504 g, 1.1 mmol) and benzene (6 mL) to give a clear, colorless solution. Me_3SiOTf (0.44 mL, 2.3 mmol) was added dropwise via syringe at room temperature, resulting in formation of a white precipitate. The reaction mixture was stirred for 20 h at ambient temperature. Removal of solvent in vacuo gave a white powder, which was washed with pentane (1 × 70 mL). Crystallization from a 1:3 THF/pentane mixture at −30 °C gave pure **7** as colorless prisms (0.609 g, 77%). ^{1}H NMR (300 MHz, THF-d_8): δ 3.80 (sept, 4H, $(CH_3)_2$C*H*, J = 6.5 Hz), 2.94 (s, 12H, (C*H*$_3)_2$N), 1.31 (s (br), 24H, (C*H*$_3)_2$CH) ppm. ^{13}C-{^{1}H} NMR (125 MHz, THF-d_8): δ 174.6 (s, N$_3$*C*), 120.4 (quart, OSO_2CF_3, J_{C-F} = 316.3 Hz), 49.7 (s (br), *C*H$(CH_3)_2$), 48.8 (s (br), *C*H$(CH_3)_2$), 40.5 (s, N(*C*H$_3)_2$), 25.0 (s (br), CH(*C*H$_3)_2$) ppm. ^{19}F NMR (376.5 MHz, THF-d_8): δ −73.1 (s, C*F*$_3$) ppm. FT-IR: 1629 (w), 1535 (s), 1407 (s), 1355 (s), 1241 (s), 1187 (s), 1131 (m), 1063 (m), 1016 (s), 985 (s), 936 (w), 747 (m), 678 (w), 635 (s) cm^{-1}. Anal. Calcd for $ZrC_{20}H_{40}N_6S_2O_6F_6$: C, 32.91; H, 5.52; N, 11.51. Found: C, 32.82; H, 5.39; N, 11.39.

(78) Brenner, S.; Kempe, R.; Arndt, P. *Z. Anorg. Allg. Chem.* **1995**, *621*, 2021.

(guan)$_2$Zr(Me)OTf (8). A 100 mL Schlenk tube was charged with **5** (0.118 g, 0.026 mmol) and hexanes (10 mL). To the resulting clear colorless solution was added via syringe a solution of Me_3SiOTf (0.057 g, 0.026 mmol) in hexanes (1.5 mL). The reaction mixture was stirred at room temperature for 4 h. Removal of solvent under reduced pressure gave crude **8** (0.124 g, 82%). Crystallization from a concentrated Et_2O solution (5 mL) at −30 °C gave pure **8** (0.072 g, 47%). ^{1}H NMR (500 MHz, C_6D_6): δ 3.51 (sept, 4H, $(CH_3)_2CH$, J = 6.5 Hz), 2.30 (s, 12H, $(CH_3)_2N$), 1.32 (d, 12H, $(CH_3)_2CH$, J = 5.5 Hz), 1.27 (d, 12H, $(CH_3)_2CH$, J = 5.5 Hz), 1.08 (s, 3H, $ZrCH_3$) ppm. ^{13}C{^{1}H} NMR (125 MHz, C_6D_6): δ 174.4 (s, N_3C), 121.0 (q, OSO_2CF_3, J_{C-F} = 317.5 Hz), 47.9 (s, $CH(CH_3)_2$), 47.3 (s, $ZrCH_3$), 40.0 (s, $N(CH_3)_2$), 25.2 (s, $CH(CH_3)_2$) ppm. ^{19}F NMR (376.5 MHz, C_6D_6): δ −77.1 (s, CF_3) ppm. FT-IR: 1531 (s), 1404 (s), 1345 (s), 1274 (m), 1237 (s), 1188 (s), 1124 (m), 1062 (s), 1002 (s), 938 (w), 747 (m), 712 (w), 6301 (s) cm^{-1}. Anal. Calcd for $ZrC_{20}H_{43}N_6F_3O_3S$: C, 40.31; H, 7.27; N, 14.10. Found: C, 40.41; H, 7.17; N, 14.34.

[(guan)$_2$ZrMe][MeB(C$_6$F$_5$)$_3$] (9). Pentane (2 mL) was added with stirring to a mixture of **5** (0.046 g, 0.010 mmol) and $B(C_6F_5)_3$ (0.051 g, 0.010 mmol). The reaction mixture was stirred at room temperature for 45 min. Removal of solvent in vacuo gave pure **9** (0.094 g, 96%) as a pale yellow viscous oil. ^{1}H NMR (500 MHz, CD_2Cl_2): δ 3.77 (sept, 4H, $(CH_3)_2CH$, J = 6.5 Hz), 2.93 (s, 12 H, $(CH_3)_2N$), 1.27 (d, 24H, $(CH_3)_2CH$, J = 6.5 Hz), 0.86 (s, 3H, $ZrCH_3$), 0.47 (br s, 3H, BCH_3) ppm. ^{13}C{^{1}H} NMR (125 MHz, CD_2Cl_2): δ 170 (s, N_3C), 147.9 (d, o-C_6F_5, J_{C-F} = 238 Hz), 137.1 (d, p-C_6F_5, J_{C-F} = 238 Hz), 136.0 (d, m-C_6F_5, J_{C-F} = 238 Hz), 128.5 (br, ipso-C_6F_5), 53.1 (s, Zr-CH_3), 48.1 (s, $CH(CH_3)_2$), 39.4 (s, $N(CH_3)_2$), 24.0 (s, $CH(CH_3)_2$), 9.5 (br, B-CH_3) ppm. ^{19}F NMR (376.5 MHz, CD_2Cl_2): δ −131.7 (d, 6F, o-C_6F_5, J_{F-F} = 21.5 Hz), −164.3 (t, 3F, p-C_6F_5, J_{F-F} = 18.4 Hz), −166.8 (t, 6F, m-C_6F_5, J_{F-F} = 18.4 Hz) ppm. ^{19}F NMR (376.5 MHz, C_6D_5Cl): δ −131.3 (d, 6F, o-C_6F_5, J_{F-F} = 21.5 Hz), −163.4 (t, 3F, p-C_6F_5, J_{F-F} = 18.1 Hz), −166.0 (t, 6F, m-C_6F_5, J_{F-F} = 18.4 Hz) ppm. ^{11}B NMR (160. 47 MHz, CD_2Cl_2): δ −15.6 (s, B-CH_3) ppm. FT-IR (neat): 2973 (s), 2936 (s), 2878 (m), 2809 (w), 1640 (s), 1544 (s), 1511 (s), 1453 (s), 1402 (s), 1336 (s), 1266 (s), 1217 (w), 1177 (s), 1125 (s), 1087 (s), 1061 (s), 952 (s), 841 (m), 749 (s), 804 (m), 710 (m) cm^{-1}. Anal. Calcd for $ZrC_{38}H_{46}N_6F_{15}B$: C, 46.87; H, 4.76; N, 8.63. Found: C, 46.59; H, 4.81; N, 8.56.

[(guan)$_2$ZrMe][B(C$_6$F$_5$)$_4$] (10). To a stirred solution of **5** (0.337 g, 0.07 mmol) in hexanes (6 mL) was added a suspension of $[Ph_3C][B(C_6F_5)_4]$ (0.673 g, 0.07 mmol) in benzene (6 mL). The reaction mixture was stirred for 1.25 h, over which time the orange color of the trityl reagent bleached, and a white solid precipitated from solution. The solvent was decanted, and the residual solid was washed with hexanes (2 × 5 mL) and dried in vacuo to give **10** as a spectroscopically and analytically pure white powder (0.760 g, 92%). ^{1}H NMR (300 MHz, C_6D_5Cl): δ 3.41 (sept, 4H, $(CH_3)_2CH$, J = 6.5 Hz), 2.46 (s, 12H, $(CH_3)_2N$), 1.02 (d, 24H, $(CH_3)_2CH$, J = 6.5), 0.72 (s, 3H, $ZrCH_3$) ppm. ^{13}C{^{1}H} NMR (125 MHz, C_6D_5Cl): δ 167.7 (s, N_3C), 146.3 (d, o-C_6F_5, J_{C-F} = 240 Hz), 136.1 (d, p-C_6F_5, J_{C-F} = 243 Hz), 134.2 (d, m-C_6F_5, J_{C-F} = 235 Hz), 51.3 (s, $ZrCH_3$), 45.9 (s, $(CH_3)_2CH$), 36.6 (s, $(CH_3)_2N$), 21.7 (s, $(CH_3)_2CH$) ppm (the ipso carbon resonance of $B(C_6F_5)_4$ was not detected). ^{19}F NMR (376.5 MHz, C_6D_5Cl): δ −131.7 (s, 8F, o-C_6F_5), −162.31 (t, 4F, p-C_6F_5, J_{FF} = 18 Hz), −166.14 (m, 8F, m-C_6F_5) ppm. ^{11}B NMR (160.47 Hz, C_6D_5Cl) δ −16.6 (s, $B(C_6F_5)_4$) ppm. FT-IR: 2727 (w), 1642 (m), 1545 (s), 1512 (s), 1412 (s), 1334 (m), 1313 (m), 1282 (m), 1176 (m), 1084 (s), 1060 (m), 981 (s), 929 (w), 842 (w), 755 (m), 683 (m), 661 (m) cm^{-1}. Anal. Calcd for $ZrC_{43}H_{43}F_{20}N_6B$: C, 45.87; H, 3.85; N, 7.46. Found: C, 46.18; H, 4.02; N, 7.54.

[((guan)$_2$ZrMe)$_2$-μ-Me][B(C$_6$F$_5$)$_4$](C$_6$H$_5$F) (11). To a stirred solution of **5** (0.278 g, 0.06 mmol) in pentane (12 mL) was added a suspension of $[Ph_3C][B(C_6F_5)_4]$ (0.278 g, 0.03 mmol) in toluene (4 mL). The reaction mixture was stirred at room temperature for 1 h, over which time the red color of the trityl reagent was bleached, and an off-white precipitate formed. The solvent was decanted, and the precipitate was washed with pentane (3 × 5 mL) and dried in vacuo to give crude **11** (0.393 g, 82%). Recrystallization of the crude product from a concentrated fluorobenzene solution at −30 °C overnight gave pure **11** (0.283 g, 56%) as colorless crystals containing 1 equiv of fluorobenzene; this material was used for characterization. ^{1}H NMR (500 MHz, CD_2Cl_2): δ 7.36 (m, 2H, C_6H_5F), 7.15 (m, 1H, C_6H_5F), 7.06 (m, 2H, C_6H_5F), 3.75 (sept, 8H, $(CH_3)_2CH$, J = 6.50 Hz), 2.86 (s, 24H, $(CH_3)_2N$), 1.20 (d, 48H, $(CH_3)_2CH$, J = 6.50 Hz), 0.71 (s, 9H, $ZrCH_3$) ppm. ^{1}H NMR (500 MHz, CD_2Cl_2, 190 K): δ 7.33 (m, 2H, o-C_6H_5F), 7.13 (t, 1H, p-C_6H_5F, J_{HH} = 7.5 Hz), 7.04 (t, 2H, m-C_6H_5F, J_{HH} = 8 Hz), 3.77 (s (br), 4H, $CH(CH_3)_2$), 3.50 (s (br), 4H, $CH(CH_3)$), 2.83 (s, 12H, $(CH_3)_2N$), 2.68 (s, 12H, $(CH_3)_2N$), 1.26 (s, 6H, $CH(CH_3)_2$), 1.19 (s, 12H, $CH(CH_3)_2$), 1.13 (s, 6H, $CH(CH_3)_2$), 1.11 (s, 3H, Zr−CH_3−Zr), 1.02 (s, 6H, $CH(CH_3)_2$), 0.79 (s, 6H, $CH(CH_3)_2$), 0.76 (s, 6H, $CH(CH_3)_2$), 0.34 (s, 6H, Zr−CH_3) ppm. ^{13}C{^{1}H} NMR (125 MHz, CD_2Cl_2): δ 174.3 (s, N_3C), 163.5 (d, ipso-C_6H_5F, J_{C-F} = 245 Hz), 148.8 (d, o-C_6F_5, J_{C-F} = 242.5 Hz), 138.8 (d, p-C_6F_5, J_{C-F} = 246.3 Hz), 136.9 (d, m-C_6F_5, J_{C-F} = 241.3 Hz), 130.6 (d, C_6H_5F, J_{C-F} = 7.5 Hz), 124.7 (d, C_6H_5F, J_{C-F} = 3.8 Hz), 115.7 (d, C_6H_5F, J_{C-F} = 21.3 Hz), 48.2 (s, $(CH_3)_2CH$), 45.7 (s, $ZrCH_3$), 40.6 (s, $(CH_3)_2N$), 25.3 (s, $(CH_3)_2CH$) ppm (ipso carbons of $B(C_6F_5)_4$ were not detected). ^{19}F NMR (376.5 MHz, C_6D_5Cl): δ −112.35 (s, 1F, C_6H_5F), −131.63 (s, 8F, o-C_6F_5), −162.44 (t, 4F, p-C_6F_5, J = 21 Hz), −166.20 (m, 8F, m-C_6F_5) ppm. ^{11}B NMR (160.47 Hz, CD_2Cl_2): δ −17.3 (s, $B(C_6F_5)_4$) ppm. FT-IR: 1642.3 (m), 1595 (w), 1514 (s), 1404(s), 1337 (s), 1274 (m), 1183 (m), 1122 (m), 1085 (m), 979 (s), 774 (m), 755 (m), 683 (w), 661 (w) cm^{-1}. Anal. Calcd for $Zr_2C_{69}H_{94}N_{12}F_{21}B$: C, 49.22; H, 5.63; N, 9.98. Found: C, 48.91; H, 5.37; N, 9.75.

[(guan)$_2$Zr(CH$_2$Ph)][B(C$_6$F$_5$)$_4$] (15). To a stirred solution of **6** (0.031 g, 0.05 mmol) in CH_2Cl_2 (1.5 mL) was added a solution of $[Ph_3C][B(C_6F_5)_4]$ (0.044 g, 0.05 mmol) in CH_2Cl_2 (1.5 mL). The reaction mixture was stirred at room temperature for 35 min. The solvent was removed under reduced pressure and the product washed with pentane (6 × 1.5 mL). Drying in vacuo gave spectroscopically and analytically pure **15** as a yellow powder (0.050 g, 88%). ^{1}H NMR (300 MHz, C_6D_5Cl): δ 3.40 (sept. 4H, $CH(CH_3)_2$, J = 6.5 Hz), 2.44 (s, 12H, $N(CH_3)_2$), 2.33 (s, 2H, $ZrCH_2Ph$), 0.91 (d, 24H, $CH(CH_3)_2$, J = 6.5 Hz) ppm (aryl protons from benzyl ligand could not be resolved due to overlap with resonances of the solvent). ^{13}C{^{1}H} NMR (125 MHz, CD_2Cl_2): δ 171.2 (s, N_3C), 148.8 (d, C_6F_5, J_{CF} = 243 Hz), 138.9 (d, C_6F_5, J_{CF} = 248 Hz), 136.9 (d, C_6F_5, J_{CF} = 244 Hz), 128.9 (s, C_6H_5), 128.5 (s, C_6H_5), 126.2 (s, C_6H_5), 77.3 (s, $ZrCH_2Ph$), 49.3 (s, $(CH(CH_3)_2)$, 40.6 (s, $(CH_3)_2N$), 25.4 (s, $(CH(CH_3)_2)$ ppm (ipso carbon resonances of C_6F_5 and C_6H_5 were not detected). ^{19}F NMR (376.5 MHz, C_6D_5Cl): δ −131.76 (s, 8F, o-C_6F_5), −162.49 (t, 4F, p-C_6F_5, J_{FF} = 21.5 Hz), −166.29 (m, 8F, m-C_6F_5) ppm. ^{11}B NMR (160.47 Hz, CD_2Cl_2): δ −17.3 (s, $B(C_6F_5)_4$) ppm. FT-IR: 1642.5 (m), 1541.0 (s), 1513.4 (s), 1410.4 (s), 1382.4 (s), 1336.2 (m), 1272.9 (m), 1176.4 (m), 1086.3 (s), 1059.1 (m), 979.1 (s), 773.9 (m), 754.5 (m), 686.2 (m), 661.7 (m) cm^{-1}. Anal. Calcd for $ZrC_{52}H_{50}F_{20}N_6B$: C, 48.97; H, 3.94; N, 6.99. Found: C, 49.10; H, 3.99; N, 6.89.

Experimental Procedure for Polymerization Experiments. All polymerization runs were carried out according to the following general procedure. The precatalyst (^{n}BuCp$_2$ZrCl$_2$, **4**, **5**, or **10**) and cocatalyst ($[Ph_3C][B(C_6F_5)_4]$, run 4 only) were dissolved in 0.50 mL of fluorobenzene. This solution was injected into a preheated (50 °C) autoclave containing 600 mL of hexane, 100−200 μmol of TIBA, 45 mL of 1-hexene (runs 1−7 only), and MMAO (runs 1−3 only). The autoclave was sealed, pressurized with ethylene, and brought up to the desired temperature. Runs 1−4 and 8 were 30 min in length; runs 5−7 were 40 min. After completion of the run, the resulting polymer was isolated by filtration and drying.

General Experimental Details for X-ray Structure Determinations. Crystals were mounted onto glass fibers using Paratone N hydrocarbon oil and were transferred to a Siemens SMART diffractometer/CCD area detector,[79] centered in the beam, and cooled by a nitrogen-flow low-temperature apparatus. Preliminary orientation matrix and cell constants were determined by collection of 60 10 or 15 s frames, followed by spot integration and least-squares refinement. A hemisphere of data was collected using ω scans of 0.3° counted for a total of 10.0 or 15.0 s per frame. The raw data were integrated by the program SAINT. Data analysis was performed using XPREP.[80] An absorption correction was applied using SADABS.[81] The unit cell parameters and statistical analysis of the intensity distribution were used for space group determination.[82] The data were corrected for Lorentz and polarization effects, but no correction for crystal decay was applied. Unique equivalent reflections were merged. The structures were solved by direct methods[83] and expanded using Fourier techniques.[84] Except as noted, all non-hydrogen atoms were refined anisotropically and hydrogen atoms were included as fixed contributions but not refined. The quantity minimized by the least-squares program was $\sum w(|F_o| - |F_c|)^2$, where w is the weight of a given observation. The weighting scheme was based on counting statistics and included a factor ($p = 0.030$) to downweight the intense reflections. The analytical forms of the scattering factor tables for the neutral atoms were used,[85] and all scattering factors were corrected for both the real and imaginary components of anomalous dispersion.[86] All calculations were performed using the teXsan[87] crystallographic software package of Molecular Structure Corp.

The carbon atoms of the disordered solvent of compound **6**, C33−C38, were refined isotropically, whereas the remaining non-hydrogen atoms were refined anisotropically. Some of the hydrogen atoms of **6** were refined isotropically; the rest were included in fixed positions. For compound **11**, the hydrogen atoms of the bridging methyl group (H1−H3) were refined isotropically, whereas other hydrogen atoms were included as fixed contributions but not refined.

Acknowledgment. We are grateful for financial support of this work from the NSF (Grant No. CHE-9633374 to R.G.B. and CHE-0072819 to J.A.). We wish to acknowledge Dr. Fred Hollander of the UC Berkeley CHEXRAY facility for determining the solid-state structure of complex **11**. We also thank Dr. Timothy Wenzel and Dr. Thomas Peterson of the Union Carbide Corp. for performing ethylene polymerization experiments, the Albemarle Corp. for generous gifts of $[Ph_3C][B(C_6F_5)_4]$ and $B(C_6F_5)_3$, and Boulder Scientific Co. for the generous gift of $[Li][B(C_6F_5)_4(Et_2O)_{2.5}]$. CNDOS is supported by Bristol-Myers Squibb as Sponsoring Member.

Supporting Information Available: Crystallographic data for compounds **1**, **4**−**7**, and **11**, including ORTEP diagrams and tables of crystal data and data collection parameters, atomic coordinates, anisotropic displacement parameters, and all bond lengths and bond angles, as well as tables summarizing $^{13}C\{^1H\}$ NMR and GPC data for the polymers produced by compounds **4**, **5**, and **10**. This material is available free of charge via the Internet at http://pubs.acs.org.

OM000995U

(79) SMART: Area-Detector Software Package; Siemens Industrial Automation, Inc., Madison, WI, 1995.

(80) XPREP (version 5.03): Part of the SHELXTL Crystal Structure Determination Package; Siemens Industrial Automation, Inc., Madison, WI, 1995.

(81) Sheldrick, G. M. SADABS: Siemens Area Detector ABSorption correction program; Advance copy, private communication, 1996.

(82) *International Tables for Crystallography*, 2nd ed.; Kluwer Academic: Boston, MA, 1989; Vol. A.

(83) Altomare, A.; Burla, M. C.; Camalli, Cascarano, M.; Giacovazzo, C.; Guagliardi, A.; Polidori, G. SIR92. *J. Appl. Crystallogr.* **1993**, *26*, 343.

(84) Beurskens, P. T.; Admiraal, G.; Beurskens, G.; Bosman, W. P.; Garcia-Granda, S.; Gould, R. O.; Smits, J. M. M.; Smykalla, C. DIRDIF: The DIRDIF Program System; Technical Report of the Crystallography Laboratory, University of Nijmegen, Nijmegen, The Netherlands, 1992.

(85) Cromer, D. T.; Waber, J. T. *International Tables for X-ray Crystallography*; Kynoch Press: Birmingham, England, 1974; Vol. IV, Table 2.2A.

(86) Creagh, D. C.; Hubbell, J. H. In I*nternational Tables for Crystallography*; Wilson, A. J. C., Ed.; Kluwer Academic: Boston, MA, 1992; Vol. C, Table 4.2.4.3, pp 200−206.

(87) teXsan: Crystal Structure Analysis Package; Molecular Structure Corp., The Woodlands, TX, 1985 & 1992.